THE JOURNAL OF PHYSICAL CHEMISTRY C

ARTICLE

pubs.acs.org/JPCC

Experimental Evidence of Local Magnetic Moments at Edges of *n*-Layer Graphenes and Graphite

Haiqing Zhou,[†,§] Huaichao Yang,[†,§] Caiyu Qiu,[†,§] Zheng Liu,[†,§] Fang Yu,[†,§] Minjiang Chen,[†,§] Lijun Hu,[†,§] Xiaoxiang Xia,[‡] Haifang Yang,[‡] Changzhi Gu,[‡] and Lianfeng Sun[*,†]

[†]National Centre for Nanoscience and Technology, Beijing 100190, China

[‡]Beijing National Laboratory for Condensed Matter Physics, Institute of Physics, Beijing 100190, China

[§]Graduate School of Chinese Academy of Sciences, Beijing 100049, China

Supporting Information

ABSTRACT: Ferromagnetism in graphite/graphenes is attractive for fundamental science and potential applications in carbon-based magnetism and spintronics. In this work, we show that magnetic particle inspection can be miniaturized to detect local magnetic moments with a high spatial resolution of ∼1.0 nm using scanning electron microscopy. A metal nanowire and adjacent nanogap can be found at the edges of graphenes and graphite for atoms with magnetic moments (Fe, Co, Ni, Mn, Pd, Al), whereas no similar characteristics are found for diamagnetic metals (Au, Ag). By investigating these features under an external magnetic field and at different temperatures, we discuss possible mechanisms and propose that intrinsic ferromagnets exist and form a one-dimensional array at the edges of graphenes and graphite. Meanwhile, the size of individual magnets (<4.8 Å), orientation, magnitude (∼0.45 μ_B per carbon edge atom) of magnetic moments, and their Curie temperature (>95 °C) are obtained, which are novel and interesting.

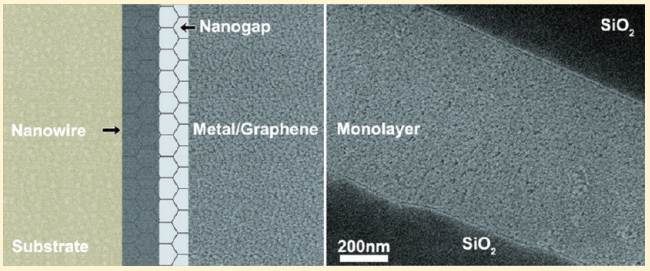

1. INTRODUCTION

Recently, experimental reports on the weak ferromagnetism of graphite[1−5] or other carbon-based materials,[6−8] which are usually assumed to be typical diamagnetic materials, have attracted great attention. Because only s/p electrons are present in carbon-based materials, which are in contrast to traditional ferromagnetic materials containing metallic 3d/4f electrons, the observation of weak ferromagnetism at room temperature or above in pure carbon-based materials has been very controversial among magnetism experts. Thus, the extremely weak signals at room temperature lead to hot debates on the physical origins of ferromagnetism in these carbon-based materials.[9−11] Meanwhile, monolayer graphene,[12] which is an individual atomic layer of graphite, with zigzag edges that are predicted to give rise to magnetic ordering.[10,11,13] According to these classical Ising[14] and Heisenberg[15] models, no long-range ferromagnetic ordering in one-dimensional systems is possible at finite temperatures. However, in these spin−lattice models,[14,15] only short-range magnetic interactions are taken into consideration, and the interactions between one-dimensional structures and their surroundings are not considered. If the interaction exists between monatomic chains of Co and a Pt substrate, long-range ferromagnetic ordering in one-dimensional monatomic chains of cobalt atoms has been found.[16] Thus, these predictions of the weak ferromagnetism in graphene or graphite need convincing experimental verifications.

In our previous work,[17] the existence of ferromagnetic ordering at the edges of *n*-layer graphenes and graphite has been recently reported. By thermally evaporating different metal films onto graphenes or graphite, we have observed that metal nanowires and adjacent nanogaps can be found for ferromagnetic (Fe, Co, and Ni) and paramagnetic (Mn, Pd, and Al) atoms at the edges of graphenes and graphite regardless of its zigzag or armchair structure, whereas no similar features for diamagnetic metals (Au and Ag). Furthermore, these features can be greatly affected by an external magnetic field, which is applied during metal evaporation. However, the size, orientation, and Curie point of local magnetic moments along the edges of graphenes and graphite are still unknown. Therefore, in this work, we aim at showing that the nondestructive testing magnetic particle inspection (MPI) widely used in the industry can be miniaturized to detect local magnetic moments. The spatial resolution is closely related to the scanning electron microscopy (SEM) used and can be as high as ∼1.0 nm, which is much higher than that of 20−50 nm reported previously.[1−4] With this technique, the following results are obtained: (1) Nanowires and adjacent nanogaps can be found clearly at the edges of graphenes or graphite for atoms with magnetic moments (ferromagnetic elements: Fe, Co,

Received: March 17, 2011
Revised: June 27, 2011
Published: July 11, 2011

ACS Publications © 2011 American Chemical Society

and Ni; paramagnetic elements: Mn, Pd, and Al). (2) By investigating these features under an external magnetic field and at different temperatures, the most plausible explanation is that intrinsic ferromagnets exist and form a one-dimensional array at the edges of graphenes and graphite. (3) The size of these magnets (distance between north and south poles) is less than 4.8 Å. (4) The orientation of the local magnetic moment is in the graphene surface and perpendicular to the edges, and its magnitude is about 0.45 μ_B per carbon edge atom. (5) The Curie temperature (T_c) of these molecular magnets can be possibly over 95 °C, which is much higher than those of single molecule magnets reported before.[18] These results open up fields of future applications of carbon-based magnetism and spintronics.[19]

In the experimental works previously reported, usually three kinds of techniques are used: MFM (magnetic force microscopy),[1−4] bulk magnetization measurements,[3−7] and XMCD (X-ray magnetic circular dichroism).[2] With the technique based on MFM, it is difficult to get quantitative results due to the lack of geometry and magnetic properties of the tip and the material under investigation. Meanwhile, to avoid the effect of long-range van der Waals forces, the tip usually works at a lift scan mode with a height of 50 nm, which causes a low spatial resolution of the location of the magnetic signal (∼20 nm). For the technique with magnetization measurements, the magnetic signals (0.0022−0.020 $Am^2 kg^{-1}$)[3,6] are extremely weak, which are 4−5 orders of magnitude smaller than those of ferromagnetic elements (∼220 $Am^2 kg^{-1}$, iron) at room temperature. Thus, it is important to know the exact contents of magnetic components[5] or to make sure that the sample is free of magnetic impurities.[3,4,6,7] XMCD is powerful to study local magnetic moments associated with different elements in a sample,[2] which can exclude the effect from magnetic impurity and have a spatial resolution of 50 nm.

2. EXPERIMENTAL METHODS

N-layer graphenes and graphite were obtained from micromechanical cleavage of natural graphite (Alfa Aesar) and then transferred onto Si substrates with a 300 nm SiO_2 layer.[20] After the layer number of *n*-layer graphenes was definitely characterized by the combined techniques (optical microscope and Raman spectroscopy), a thin metal film (ferromagnetic elements: Fe, Co, Ni; paramagnetic elements: Mn, Pd, Al; diamagnetic elements: Au and Ag) was thermally evaporated onto the wafer in a vacuum thermal evaporator with the substrate keeping at controlled temperature or with an external magnetic field produced by a permanent NdFeB magnet, respectively (Figure 1 and the Supporting Information, Figure S1).

Fe (99.99%) was bought from Alfa Aesar, and Co (99.75%) and Ni (99.99%), were bought from the General Research Institute for Nonferrous Metals, Beijing, China. These metals were evaporated onto the wafer in a vacuum thermal evaporator at a deposition rate of 1.0 Å/s under a vacuum of 10^{-4} Pa. To keep the substrate at a temperature higher than room temperature, the wafer was fixed to the ceramic mounting surface of a power film resistor (MP9100) by carbon adhesive tape. When a permanent magnet was applied, the wafer and the magnet were mounted on an aluminum stage with the graphene at a position of known magnetic field.

The layer number of *n*-layer graphenes was identified using the combination of an optical microscope (Leica DM 4000) and micro-Raman spectroscopy (Renishaw inVia Raman Spectroscope). The detail of Raman measurements is shown in the Supporting Information. After different metal films were thermally deposited onto *n*-layer graphenes or graphite, a scanning electron microscope (SEM) was used to characterize the film morphologies at the edges of *n*-layer graphenes or graphite. When the substrate was kept at a controlled temperature or an external magnetic field was applied upon thermal deposition, the orientation, magnitude, and the corresponding Curie temperature of the local magnetic moment at the edge of *n*-layer graphenes or graphite can be determined according to the changes in film morphologies.

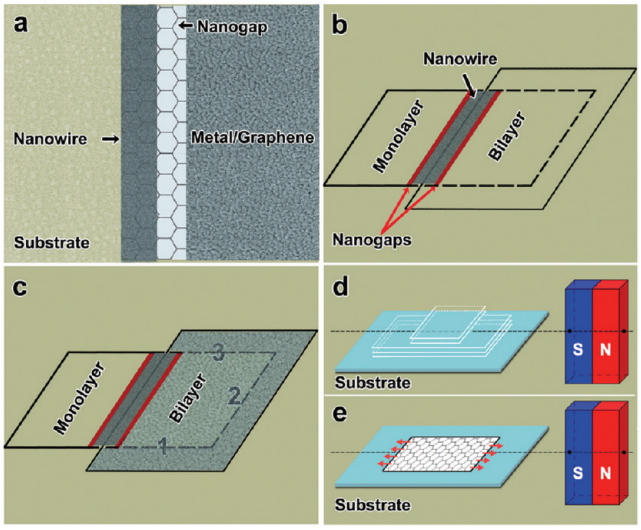

Figure 1. Diagrams showing the technique to demonstrate the existence and characteristics of ferromagnets at the edges of graphenes or graphite. The sizes are not in scale for clarity. (a) The appearance of a metal nanowire and adjacent nanogap at and on the edges of graphenes for atoms with magnetic moments (Fe, Co, Ni, Mn, Pd, Al). (b) A nanowire and two adjacent nanogaps found at the edge of the upper monolayer graphene. (c) No aggregation of atoms at the edges ("1′′, "2", "3") of the lower monolayer graphene. (d) The orientation of the magnetic moment at the edges of graphene and graphite determined by different changes of morphologies of the metal film at the left and right sides under an external magnetic field. (e) The magnitude of the magnetic moment of monolayer graphene obtained from the disappearance of the nanogap and/or nanowire at the left edge where the external field cancels with the local one.

3. RESULTS AND DISCUSSION

In this work, a different technique is used, which is a miniature implementation of the nondestructive testing magnetic particle inspection (MPI) widely used in the industry (Figure 1). As shown in the schematic diagram of Figure 1, after ferromagnetic or paramagnetic metals are thermally deposited onto *n*-layer graphenes and graphite, we can determine the size, orientation, magnitude, and the corresponding Curie temperature accordingly. First, for atoms with magnetic moments (Fe, Co, Ni; Mn, Pd, Al), a metal nanowire and adjacent nanogap at and on the edges of graphenes can be observed under SEM (Figure 1a), whereas no similar features are found for diamagnetic metals (Au and Ag). This indicates the existence of intrinsic magnetic moments at these locations, resulting in the aggregation of atoms with magnetic moments (Fe, Co, Ni; Mn, Pd, Al) at the edges of graphenes.[17] Second, when two monolayer graphenes stack together, the edge of the upper graphene (terraced edge) can

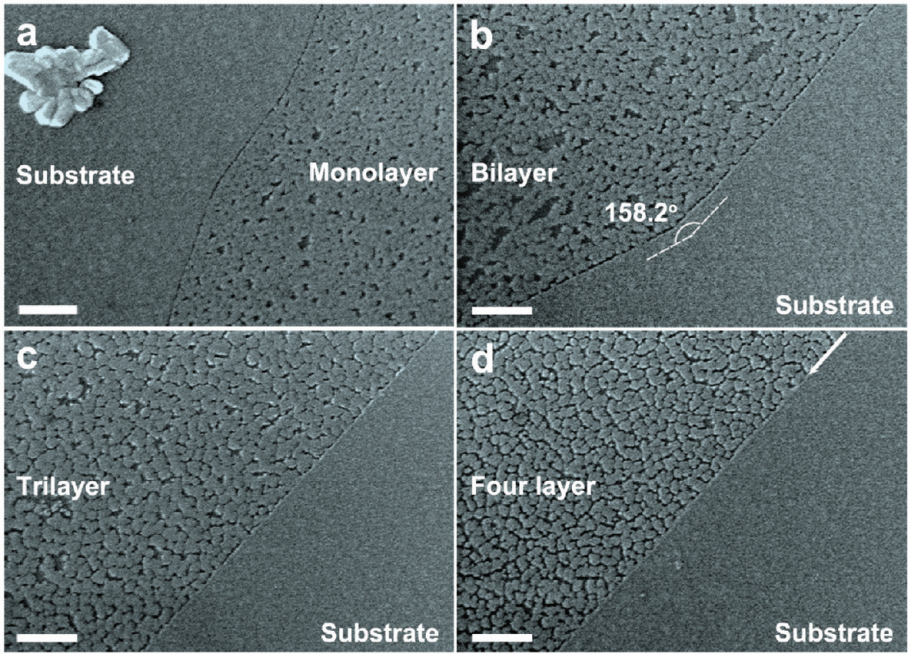

Figure 2. SEM images of Fe nanowires and adjacent nanogaps at the edges of *n*-layer graphenes. Film thickness: 2.0 nm. Scale bar: 200 nm. (a) Monolayer graphene and substrate (SiO_2). (b) Bilayer graphene and substrate. The angle is 158.2°. (c) Trilayer graphene and substrate. (d) Four-layer graphene and substrate.

be in direct contact with metal atoms (Figure 1b). Atoms with magnetic moments can be attracted to aggregate from both sides. Thus, a nanowire and two adjacent nanogaps can be found along this edge. Third, as shown in Figure 1c, the edges ("1", "2", "3") of the lower monolayer graphene cannot be in direct contact with the evaporated atoms. We can find that no aggregation of atoms on the above corresponding graphenes is found. This implies that the magnetic field produced by this edge is perpendicular to the upper graphene surface, from which the size of the magnets can be obtained. Additionally, when an external magnetic field is applied, after metal film deposition, the different changes in morphologies of the metal film at the left and right sides can be observed (Figure 1d). Thus, we can determine the orientation of the local magnetic moments at the edges of *n*-layer graphenes and graphite. Finally, according to Figure 1e, the local one at the left or right edge of monolayer graphene can be canceled or enhanced by the external magnetic field, so the disappearance of the nanogap and/or nanowire can help us to estimate the magnitude of local magnetic moments at the edge of monolayer graphene. Note that the films of metal on other parts of graphenes and substrate are not shown in Figure 1b,c. The arrows in Figure 1e indicate the orientation of local magnetic moments.

As shown in Figure 2, the morphologies of the iron film on graphenes can be greatly related to the layer number of *n*-layer graphenes: with the increase of the layer number, the size of a single iron grain becomes larger, and the iron film rougher. These phenomena are very similar to those of gold on graphenes reported by Luo and Zhou et al.[20,21] Meanwhile, similar to nickel films at the edges of *n*-layer graphenes, the following features can be seen clearly: there is a nanogap of iron along the edge of *n*-layer graphenes (n = 1, 2, 3, 4), which separates the central iron films from those along the edge of graphenes. These features can also be found at the edges of *n*-layer graphenes (n = 1, 2, 3, 4), which are independent of the kinds of edges: straight or at angles (Figure 2a−d).

Different from nickel films at the edge of graphenes (Figure 3a,b), it is not obvious that Fe (Co) nanowires are clearly observable at the edges of monolayer, bilayer, and trilayer graphenes (Figures 2a−d and 3c,d). However, the existence of these nanowires at the edge of graphenes can be justified from the following reasons: First, the nanogaps are clearly observed between *n*-layer graphenes and substrate (n = 1, 2, 3; Figures 2a−c and 3c,d and the Supporting Information, Figure S2). Second, the nanowires (aggregation) of Fe (Co) at terraced edges are obvious (Figure 3c,d). Third, the nanowire of iron at the edge of four-layer graphene can be clearly observed, as shown by the white arrow in Figure 2d. The reason that the nanowires of Fe (Co) at the edges of *n*-layer graphenes (n = 1, 2, 3) cannot be clearly observed under SEM is believed to result from the low contrast of these nanowires with those metallic films on the silicon substrate.

The thermodynamic (e.g., energetics and stability) and kinetic (e.g., surface diffusion) factors can well account for the thickness-dependent morphologies of iron on the central area of *n*-layer graphenes, which is analogous to the situation of gold.[20,21] The quite interesting result here is why the iron morphologies at the edges of graphenes are so unique and different? To figure out the mechanism, other ferromagnetic, paramagnetic, or diamagnetic elements have been deposited onto graphenes and graphite, such as Ni, Co (ferromagnetic elements), Mn, Pd, Al (paramagnetic metals), Au, and Ag (diamagnetic metals), respectively.[17] As is reported, for ferromagnetic (Fe, Co, and Ni) or paramagnetic (Mn, Pd, and Al) metals, there is a nanowire and adjacent nanogap at the edges of *n*-layer graphenes (n = 1, 2, 3).

Especially in Figure 3, when graphenes with different numbers of layers stack together, there are two kinds of edges: edges of the upper graphenes that can be in direct contact with evaporated nickel atoms (terraced edges) and edges of the lower graphenes

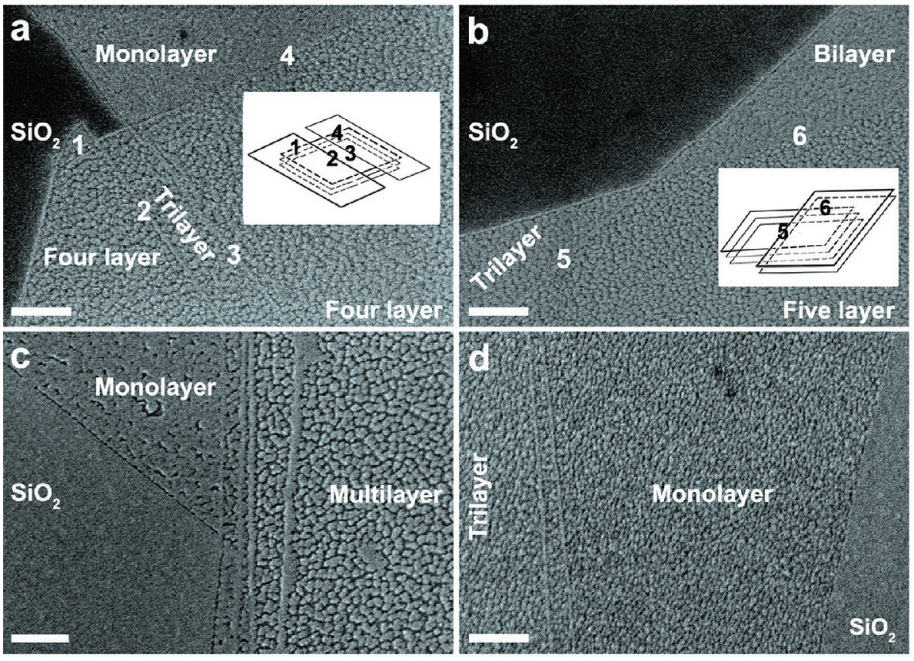

Figure 3. SEM images of Ni, Fe, and Co films on the graphene surface at 25 °C. Scale bar: 200 nm. Thickness: 2.0 nm. (a) Ni on the stacked layers of a trilayer with two monolayer graphenes, as schematically shown in the inset. (b) Ni on the stacked layers of a bilayer with a trilayer graphene, as schematically shown in the inset. (c) Fe on monolayer graphene stacked with thicker graphenes. (d) Morphologies of cobalt film on *n*-layer graphenes (n = 1, 2, 3) and substrate.

that cannot be in direct contact with nickel atoms (Figure 3a,b). Different features of the nickel film can be found in these two kinds of edges, such as those marked with "1", "2", "3", "4", "5", and "6" in Figure 3a,b. Here, the nickel films at "2′′", "3", and "5" appear as individual nanowires that are separated from both sides by nanogaps. The formation of nanowires along these edges implies the aggregation of nickel atoms at these locations, and these edges can be identified as those of the upper graphenes (terraced edges). Correspondingly, the nickel films at "1", "4", and "6" have morphologies between those of either sides and the edges can be identified as edges of the lower graphenes. Meanwhile, for Fe and Co, similar features can also be observed at terraced edges between graphenes with different layer numbers (Figure 3c,d). It is concluded that a metal nanowire and adjacent nanogap can be definitely found for ferromagnetic (Fe, Co, and Ni) or paramagnetic elements (Mn, Pd, Al)[17] at the edges of graphenes or at terraced edges (Figures 2 and 3), which can be mainly attributed to the attraction and aggregation of atoms with magnetic moments,[17] rather than the short-ranged strong chemical forces at the edges of graphenes,[22] indicating the existence of intrinsic magnetic moments at the edges of graphenes, which can be further confirmed by the EDX analysis at the edge of graphite (Supporting Information, Figure S3).

Although the magnetic potential energy changes in a magnetic field experienced by an adatom (∼1 Bohr magneton) on graphenes are about 3 orders of magnitude below KT at room temperature, we think it is reasonable for the extension of the MPI to nanoscale. First, when adatoms diffuse on graphenes, which is thermally activated, the motion is two-dimensional, random, and nondirectional. A nonuniform magnetic field can make the adatoms have a directional movement even if the magnetic potential energy changes are small. This directional movement results in the accumulation and aggregation of adatoms at the edges of graphenes. This mechanism has an analogy to that in the well-known Hall Effect.[23] For metals, the Hall voltage has a typical value of tens of microvolts, which depends on the current and magnetic field. Thus, the electrical potential is about tens of microelectron volts ($\sim 10^{-5}$ eV, Hall voltage times the c harge of an electron), which is 3 orders of magnitude below KT ($\sim 2.5 \times 10^{-2}$ eV) at room temperature. As shown in Figure S6 (Supporting Information), the mechanism of Hall voltage is the accumulation of electrons at two opposite sides. Second, the force on a magnetic moment by a nonuniform magnetic field is proportional to the gradient of this field. For the applied external magnetic field by the NdFeB magnet, the gradient is about 35 T/m. This magnetic field has a significant effect on the process of diffusion, aggregation of adatoms, and the final morphologies of the metal film (Figure 4b,d,e and the Supporting Information, Figures S4 and S5). Third, as estimated and discussed below, the gradient of the local magnetic field at the edges of graphenes is $\sim 1.75 \times 10^{7}$ T/m, which is about 6 orders of magnitude higher than that of the macro NdFeB magnet.

The formation of nanowires and adjacent nanogaps at straight or curved edges suggests that the orientation of the magnetic moment should be in the plane of graphenes and perpendicular to the edges. This is confirmed by the experiments with an external magnetic field in the $\pm z$ direction (Supporting Information, Figure S7). Similar morphologies of iron can be found for external fields in the $\pm z$ direction, indicating that the orientation of the local magnetic moment is in the plane of monolayer graphene. Otherwise, an external magnetic field in the $+z$ direction should cause different morphologies from that in the $-z$ direction because only one directional external field will counteract the local magnetic field.

If an external magnetic field parallel to the surface is applied (Figure 1d), the orientation of local magnetic moments can be

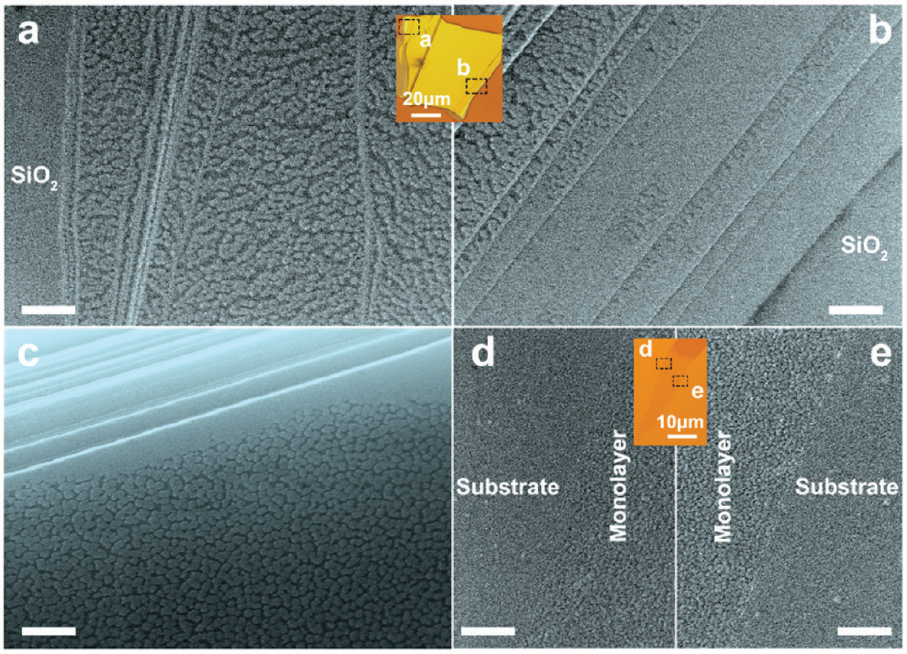

Figure 4. SEM images of the Fe film at the edges of graphite and graphenes with and without an external magnetic field at 25 °C. Scale bar: 200 nm. Thickness: 2.0 nm. (a, b) Iron at the left and right sides of a graphite flake with an external magnetic field, respectively (magnitude, 0.32 T; direction, left to right). The inset is the corresponding optical image. (c) Iron film at the edges of a graphite flake without a magnetic field. (d, e) Iron film on monolayer graphene at its left and right edges with the application of an external magnetic field, respectively (direction, left to right; magnitude, 0.35 T). The inset is the corresponding optical image of monolayer graphene.

obtained by the changes of morphologies at two opposite sides of graphite. After the application of an external field (direction: left to right), the morphologies of iron at the left side of graphite have changed significantly (Figure 4a). Compared to the uniform and smooth iron film at the edges of graphite without an external field (Figure 4c), iron nanowires and nanocrystals form at terraced edges and on central surfaces at the left side of graphite, respectively (Figure 4a). For the right side (Figure 4b), the iron atoms form a film with similar features to that of Figure 4c. These results indicate that the orientation of the local magnetic moments at the edges is in the surface of graphenes and pointing outward.

It is difficult to obtain the magnitude of local magnetic moments using terraced edges in multilayer graphenes or graphite because the morphologies of the iron film are sensitive to the thickness of terrace edges, the external field, etc. If iron is evaporated onto monolayer graphene with an external field of appropriate strength, the external field (left to right) will cancel with the local field of the left edge, which can be judged from the disappearance of the nanogap (Figure 2a). We can see clearly from Figure 4d that the nanogap at the left edge disappears under an external field of 0.35 T, indicating the same field strength by the local magnetic moment. Thus, the magnetic moment can be estimated based on the following calculations (Supporting Information, Part 7): As is discussed above, the orientation of the local magnetic moments is parallel to the graphene surface and perpendicular to the edges, which is designated as the z direction, and the middle of the local magnetic moment as the (0, 0, 0) point. Correspondingly, the x axis is designated as being perpendicular to the graphene plane. Considering the magnetic field produced by a magnetic moment,[24,25] the magnetic field at (0, 0, z_0) produced by one-dimensional arrays of magnetic moments along the y axis can be obtained by the following integral

$$B_z = \int_{+\infty}^{-\infty} \frac{\mu_0}{4\pi} \times 3M \times \frac{z_0^2 - \frac{1}{3}(y^2 + z_0^2)}{(y^2 + z_0^2)^{5/2}} \mathrm{d}y$$

$$= \frac{\mu_0}{4\pi} \times 3M \times \left[\frac{y}{3(y^2 + z_0^2)^{3/2}} + \frac{1}{3} \times \frac{y}{z_0^2 \times \sqrt{y^2 + z_0^2}} \right] \Big|_{-\infty}^{+\infty}$$

$$= \frac{\mu_0}{4\pi} \times 3M \times \frac{2}{3z_0^2}$$

we can obtain the following equation: $B_z(0, 0, z_0) = [\mu_0/(4\pi)] \times 3M \times [2/(3z_0^2)] = 0.35$ T, where μ_0 is vacuum permeability, M the linear magnetic moment density, and z_0 the size of the local magnetic moment (2.4 Å). Thus, the linear magnetic moment density (M) can be obtained as $M = 1.01 \times 10^{-13}$ Am^2/m, and the magnetic moment can be calculated, which is about 0.45−0.46 μ_B per edge carbon atom and comparable to that of nickel at room temperature (~0.57 μ_B) (Supporting Information, Figure S8). Meanwhile, the nanogap at the right edge of the monolayer graphene also disappears, although the local magnetic field is in the same direction with the external field (Figure 4e). Possible reasons include the following: First, the iron atoms are attracted and deflected in the vacuum before they arrive at the surface of graphene due to the long-range force of the nonuniform external field. Second, after the application of an external field, the adatoms diffuse on the surface of monolayer graphenes

dx.doi.org/10.1021/jp202540a |J. Phys. Chem. C 2011, 115, 15785–15792

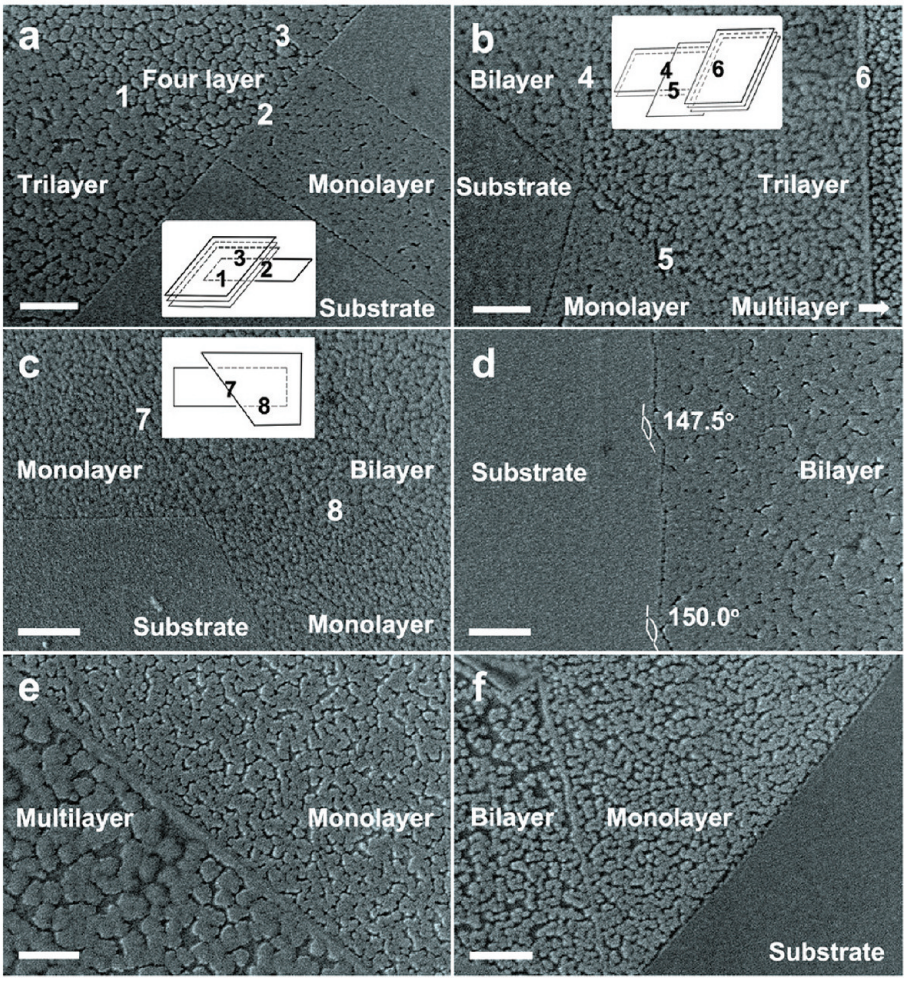

Figure 5. SEM images of Fe film on *n*-layer graphenes in the temperature range from 25 to 95 °C. (a, b) Stacked graphenes with different numbers of layers (insets: illustration of the stacking). Temperature: 25 °C. Thickness: 2.0 nm. (c) Stacking of two monolayer graphenes. Temperature: 35 °C. Thickness: 2.6 nm. (d) Bilayer graphene and substrate at 55 °C. Thickness: 2.8 nm. (e) Monolayer and multilayer graphene at 75 °C. Thickness: 3.0 nm. (f) Monolayer, bilayer graphene, and substrate at 95 °C. Thickness: 3.2 nm.

differently, which results in different morphologies of the iron film on monolayer graphenes, as shown in Figure S4 (Supporting Information).

On the basis of the above discussions, the mechanism of the formation of nanowires and an adjacent nanogap can be explained in detail as follows: When atoms with magnetic moments are thermally deposited onto the boundary area between graphenes and substrate (SiO_2), these adatoms will be attracted by the nonuniform magnetic field produced by the magnetic moments at the edges of graphenes. Because of the extremely high gradient of this local field (~0.35 T/20 nm = 1.75 × 10^7 T/m) and different surface diffusion coefficients[20,21] on graphenes and SiO_2, a metal nanowire and an adjacent nanogap can be observed at and on the edges of graphenes under SEM (Figures 1a, 2d, 3, and the Supporting Information, Figure S2). For terraced edges between graphenes, the magnets at the edge will attract atoms from both sides, which results in a nanowire and two adjacent nanogaps at these edges (Figure 1b and edges "2", "3", and "5" in Figure 3a,b). When the edges locate underneath (insets in Figure 3a,b), such as "1", "4 ", and "6", the evaporated atoms diffuse on the surface of the upper graphenes, and no metal nanowires/nanogaps can be found at these locations. The absence of obvious aggregation of atoms suggests that the local magnetic field produced by the underneath edges is perpendicular to the upper graphene surface. Thus, the size of these magnets (the length between the north and south poles) can be estimated, which is less than 4.8 Å, and these magnets are named molecular magnets (Supporting Information, Figure S9). The above results indicate that only a tiny fraction of the carbon atoms at the edge will contribute to bulk magnetization measurements. By assuming a size of several tens of nanometers and a random orientation of individual graphenes in the bulk sample, we can estimate the bulk magnetization and compare with those reported previously,[3,6] which are quite consistent (Supporting Information).

Another interesting, unexpected observation is the existence of ferromagnetic ordering at the edges of graphenes or graphite no matter what kinds of the edges there are: straight, curved,[17] or at angles (Figure 2). Theoretical calculations predict that ferromagnetism may exist only in graphenes with zigzag edges.[9,13] It is not possible that all the edges are zigzag because there are angles of odd multiples of 30° (Figure 2b), which indicates that the two edges of these angles have different chiralities, that is, one armchair and the other zigzag[26,27] (Supporting Information, Figure S10). This contradiction may be resolved in this way:

Theoretical calculations usually assume ideal graphene edge structures, armchair or zigzag. In experiments, however, the edges of graphene may exist atomic roughness. For example, there are experimental works published recently[28,29] that indicate the possibility of an irregular edge structure of graphenes. The correlation of edge structure with ferromagnetism needs more theoretical and experimental works for future studies.

One important property of a ferromagnetic material is the existence of the Curie point (T_c). In search of the T_c of these molecular magnets, experiments are carried out with the substrate kept at temperatures in the range of 25−95 °C (Figure 5). We can see clearly that the morphologies of iron on graphenes change with temperature, which should result from the changes in surface free energies and diffusion rates of the metals.[20,21] However, the important features, such as the nanogaps and the iron nanowires at the edges of graphenes and at terraced edges, can always be observed in the temperature range studied (Figure 5). From the aggregation of Fe atoms at the terraced edges, we can easily conclude that, in Figure 5a,b, edges "2", "4", and "6" can be the terraced ones, whereas edges "1″", "3", and "5" locate underneath and are covered by trilayer and monolayer graphene, respectively. Especially in Figure 5c, Fe nanowire and adjacent nanogaps can be seen at terraced edge "7", while no obvious aggregation of iron atoms on the upper monolayer graphene along edge "8", indicating that this edge is located underneath and covered by the other monolayer graphene. The absence of iron atom aggregation may suggest that the magnetic field produced by edge "8" is perpendicular to the surface of the upper monolayer graphene, from which the size of the magnet can be estimated (Supporting Information, Figure S9). Here, according to the magnetic field produced by local magnetic dipole moments,[24,25] for the upper monolayer graphene (Figure 5c), the magnetic field produced by the local magnetic moments at the edge of lower monolayer graphene is perpendicular to the surface of the upper monolayer graphene (Supporting Information, Part 8), and the z component at this point $(d, 0, z_0)$ should satisfy this equation: $B_z(d, 0, z_0) = [\mu_0/(4\pi)] \times 3M \times \{[z_0^2 - (1/3)(d^2 + 0 + z_0^2)]/[(d^2 + 0 + z_0^2)^{5/2}]\} = 0$, where μ_0 is the vacuum permeability, M the magnetic moment, and $d = 0.34$ nm (interlayer spacing). Therefore, the size of the local magnets is around 2.4 Å. Meanwhile, the Fe nanowire (aggregation of iron atoms) at the terraced edge (Figure 5f) can be still seen clearly, suggesting that ferromagnetic order still exists at this temperature and T_c is over 95 °C (Supporting Information, Figure S11), which is much higher than that of molecular magnets reported previously.[18]

The magnetic proximity effect, a net transfer of spins of electrons when graphite comes into contact with ferromagnetic metals, has been proposed previously.[5,30,31] Although this effect can explain the results for Ni, Fe, and Co, it is not applicable here and can be excluded by the observations with paramagnetic elements (Mn, Pd, and Al) or diamagnetic elements (Au and Ag).[17,31] It should be noted that the existence of a one-dimensional magnet seems to be contrary to Ising[14] and Heisenberg[15] models, which prohibit long-range ferromagnetic order in a one-dimensional linear chain at a finite temperature. However, in these spin−lattice models, the assumptions of short-range magnetic interactions and no interactions with its surroundings are important for these conclusions.[5,14,15] We believe that these assumptions are not applicable because the central parts of graphenes play important roles for the existence and high Curie point of one-dimensional ferromagnetism at the edges of graphenes.

4. CONCLUSIONS

We have provided evidence to show that intrinsic local magnetic moments exist at the edges of gaphenes and graphite by using miniaturized magnetic particle inspection. These magnets form a one-dimensional array and have a smaller size (<4.8 Å) and a Curie point over 95 °C. The magnetic moment is about 0.45−0.46 μ_B per carbon edge atom, which implies that carbon is the fourth ferromagnetic element with a Curie point above room temperature besides Fe, Co, and Ni.[32,33]

■ ASSOCIATED CONTENT

Ⓢ Supporting Information. The magnetic field of permanent NdFeB magnets used in the experiments, Fe film morphologies on partially split trilayer graphene, EDX analysis at the edges of graphite, comparison of morphologies of Fe (Pd) film on graphenes between with and without an external magnetic field, the mechanism of the accumulation of electrons in the Hall effect in metals, graphenes covered with iron under perpendicular magnetic fields, calculation of the magnetic moment per carbon edge atom, estimation of the size of the molecular magnets and bulk magnetization, Raman spectra at the edges of graphenes, and estimation of the Curie point. This material is available free of charge via the Internet at http://pubs.acs.org.

■ AUTHOR INFORMATION

Corresponding Author

*E-mail: slf@nanoctr.cn. Telephone: 86-10-82545584. Fax: 86-10-62656765.

■ ACKNOWLEDGMENT

This work was supported by National Science Foundation of China (Grant Nos. 10774032, 90921001, 50825206).

■ REFERENCES

(1) Han, K. H.; Spemann, D.; Esquinazi, P.; Hohne, R.; Riede, V.; Butz, T. *Adv. Mater.* **2003**, *15*, 1719.
(2) Ohldag, H.; Tyliszczak, T.; Höhne, R.; Spemann, D.; Esquinazi, P.; Ungureanu, M.; Butz, T. *Phys. Rev. Lett.* **2007**, *98*, 187204.
(3) Cervenka, J.; Katsnelson, M. I.; Flipse, C. F. J. *Nat. Phys.* **2009**, *5*, 840.
(4) Esquinazi, P.; Spemann, D.; Höhne, R.; Setzer, A.; Han, K. H.; Butz, T. *Phys. Rev. Lett.* **2003**, *91*, 227201.
(5) Coey, J. M. D.; Venkatesan, M.; Fitzgerald, C. B.; Douvalis, A. P.; Sanders, I. S. *Nature* **2002**, *420*, 156.
(6) Wang, Y.; Huang, Y.; Song, Y.; Zhang, X. Y.; Ma, Y. F.; Liang, J. J.; Chen, Y. S. *Nano Lett.* **2009**, *9*, 220.
(7) Makarova, T. L.; Sundqvist, B.; Höhne, R.; Esquinazi, P.; Kopelevich, Y.; Scharff, P.; Davydov, V.; Kashevarova, L. S.; Rakhmanin, A. V. *Nature* **2001**, *413*, 716. Retraction: *Nature* **2006**, *440*, 707.
(8) Service, R. F. *Science* **2004**, *304*, 42.
(9) Zhang, Z. H.; Chen, C. F.; Guo, W. L. *Phys. Rev. Lett.* **2009**, *103*, 187204.
(10) Kou, L. Z.; Tang, C.; Guo, W. L.; Chen, C. F. *ACS Nano* **2011**, *5*, 1012.
(11) Radovic, L. R.; Bockrath, B. *J. Am. Chem. Soc.* **2005**, *127*, 5917.
(12) Novoselov, K. S.; Geim, A. K.; Morozov, S. V.; Jiang, D.; Zhang, Y.; Dubonos, S. V.; Grigorieva, I. V.; Firsov, A. A. *Science* **2004**, *306*, 666.

(13) Lu, P.; Zhang, Z. H.; Guo, W. L. *Phys. Lett. A* **2009**, *373*, 3354.
(14) Ising, E. *Z. Phys.* **1925**, *31*, 253.
(15) Mermin, N. D.; Wagner, H. *Phys. Rev. Lett.* **1966**, *17*, 1133.
(16) Gambardella, P.; Dallmeyer, A.; Maiti, K.; Malagoli, M. C.; Eberhardt, W.; Kern, K.; Carbone, C. *Nature* **2002**, *416*, 301.
(17) Zhou, H. Q.; Yang, H. C.; Qiu, C. Y.; Liu, Z.; Yu, F.; Hu, L. J.; Xia, X. X.; Yang, H. F.; Gu, C. Z.; Sun, L. F. *Chin. Phys. B* **2011**, *20*, 026803.
(18) Gatteschi, D.; Sessoli, R. *Angew. Chem., Int. Ed.* **2003**, *42*, 268.
(19) Leuenberger, M.; Loss, D. *Nature* **2001**, *410*, 789.
(20) Zhou, H. Q.; Qiu, C. Y.; Liu, Z.; Yang, H. C.; Hu, L. J.; Liu, J.; Yang, H. F.; Gu, C. Z.; Sun, L. F. *J. Am. Chem. Soc.* **2010**, *132*, 944.
(21) Luo, Z. T.; Somers, L. A.; Dan, Y. P.; Ly, T.; Kybert, N. J.; Mele, E. J.; Johnson, A. T. C. *Nano Lett.* **2010**, *10*, 777.
(22) Chan, K. T.; Neaton, J. B.; Cohen, M. L. *Phys. Rev. B* **2008**, *77*, 235430.
(23) Hall, E. H. *Am. J. Math.* **1879**, *2*, 287.
(24) Schill, R. A. *IEEE Trans. Magn.* **2003**, *39*, 961.
(25) Boyer, T. H. *Am. J. Phys.* **1988**, *56*, 688.
(26) Warner, J. H.; Schaffel, F.; Rummeli, M. H.; Buchner, B. *Chem. Mater.* **2009**, *21*, 2418.
(27) You, Y. M.; Ni, Z. H.; Yu, T.; Shen, Z. X. *Appl. Phys. Lett.* **2008**, *93*, 163112.
(28) Jia, X. T.; Hofmann, M.; Meunier, V.; Sumpter, B. G.; Campos-Delgado, J.; Romo-Herrera, J. M.; Son, H.; Hsieh, Y. P.; Reina, A.; Kong, J.; Terrones, M.; Dresselhaus, M. S. *Science* **2009**, *323*, 1701.
(29) Warner, J. H.; Rümmeli, M. H.; Ge, L.; Gemming, T.; Montanari, B.; Harrison, N. M.; Büchner, B.; Briggs, G. A. D. *Nat. Nanotechnol.* **2009**, *4*, 500.
(30) Uchoa, B.; Yang, L.; Tsai, S. W.; Peres, N. M. R.; Neto, A. H. C. *Phys. Rev. Lett.* **2009**, *103*, 206804.
(31) Céspedes, O.; Ferreira, M. S.; Sanvito, S.; Kociak, M.; Coey, J. M. D. *J. Phys.: Condens. Matter* **2004**, *16*, L155.
(32) Weller, T. E.; Ellerby, M.; Saxena, S. S.; Smith, R. P.; Skipper, N. T. *Nat. Phys.* **2005**, *1*, 39.
(33) Kamihara, Y.; Hiramatsu, H.; Hirano, M.; Kawamura, R.; Yanagi, H.; Kamiya, T.; Hosono, H. *J. Am. Chem. Soc.* **2008**, *130*, 3296.